A Modified Redundancy-Based Energy Management System for Microgrids

An SoC Enhancement Approach

Fagundes, Thales Augusto; Fuzato, Guilherme Henrique Favaro; Magossi, Rafael Fernando Quirino; Silva, Lucas Jonys Ribeiro; Vasquez, Juan C.; Guerrero, Josep M.; Machado, Ricardo Quadros

Published in:
IEEE Transactions on Industrial Electronics

DOI (link to publication from Publisher):
10.1109/TIE.2023.3342325

Publication date:
2024

Document Version
Accepted author manuscript, peer reviewed version

A Modified Redundancy-Based Energy Management System for Microgrids: An SoC Enhancement Approach

Thales Augusto Fagundes, Guilherme Henrique Favaro Fuzato, *Member, IEEE*, Rafael Fernando Quirino Magossi, Lucas Jonys Ribeiro Silva, Juan C. Vasquez, *Senior Member, IEEE*, Josep M. Guerrero, *Fellow, IEEE*, and Ricardo Quadros Machado, *Senior Member, IEEE*

***Abstract*—This paper proposes a dc microgrid (MG) composed by a cascaded bidirectional Cuk converter (CBC) connected to a cascaded bidirectional Boost converter (CBB) sharing two battery energy storage systems (BESSs) as common inputs. Then, the dc-link from CBC also receives a Boost converter which interfaces the dc-utility. Thus, this configuration can coordinate the BESSs and the dc-utility by employing the state-of-charge (SoC)-sharing function and droop controller. In this context, the combination between CBC and CBB can improve the reliability of the SoC-sharing function with the battery-to-battery (B2B) equalization on CBB and can enhance the availability of power production on the CBC dc-link. Therefore, the main advantage of the proposed method is to ensure the SoC equalization even when the MG is under maintenance or electrical fault. Additionally, the dc MG involves a modified energy management system (EMS), while the Lyapunov's indirect method proves the stability analysis. Finally, the experimental setup validates the feasibility of the proposed approach.**

***Index Terms*—battery energy storage system (BESS), Cascaded bidirectional Boost converter (CBB), Cascaded bidirectional Cuk converter (CBC), energy management system (EMS), state-of-charge (SoC) equalization.**

I. Introduction

THE employment of battery energy storage systems (BESSs) has been increased in coordination with non-predictable renewable energy sources (RES) in dc microgrids (MGs) [1]. Thus, the BESSs can guarantee that the final energy consumers have their local demand provide from the dc MG even though the RES are facing low electricity production due to weather conditions [2], [3]. In addition, when a fuel cell is also included in the dc MG, a BESS can also be important to suppress or absorb load transients from the dc-link and avoid damages on its membrane [4].

The integration of BESSs offers various advantages but can also present some challenges, such as the replacement of aging devices, isolation of fault modules and compensation of load transient can result in unbalanced SoCs when the BESSs are integrated in a MG [5], [6]. As a result, several strategies have been discussed to increase their operation, then, to prevent deep discharge or over-charge, the coordination among the sources and BESSs is required [7]. Failure to do so may result in a reduction of the BESSs life-cycle and overall degradation, thus, the balancing of the state-of-charge (SoC) is essential to avoid different rates of charge/discharge that can lead them to further damage [8], [9]. The most effective solution to improve the operation of the dc MG is related to an intelligent control structure that can speed up the charge and minimize disparate wear and tear in BESSs [10]. Different equalization strategies, such as the solutions based on the SoC, voltage, or BESS capacity can be implemented to ensure the SoCs balancing and the protection of individual BESSs [11].

In [12]–[14], a set of dc/dc converters to balance the SoCs among the battery cells was proposed, while [15]–[19] worked in the SoC equalization among BESSs connected to the dc MG via bidirectional dc/dc converter. Aiming at the SoC balancing among the BESSs, [15] proposed a strategy considering the product of SoC and Ampere-hour (Ah) rating (reflected Ampere-hour capacity), while [16] elaborated a coordination among BESSs by using the Fuzzy logic which can balance their SoCs. In [17], [18], [20], [21] an SoC-based droop can achieve the same performance, while [19] applied an adaptive droop control implemented in partnership with the Fuzzy logic.

The common structure of a dc MG that operates with BESSs is composed by the bidirectional dc/dc converters in parallel connection [15]–[20], while the unbalanced SoC among BESSs is solved with a strategy by using a modular multilevel converter in [5] for shipboard applications. However, redundancy is important to avoid problems with navigation

This work was supported by the Coordination for the Improvement of Higher Education Personnel (CAPES) under grants PDSE-88881.187771/2018-01, 88881.030370/2013-0 and 88887.482911/2020-00, the National Council for Scientific and Technological Development (CNPq) under grant 309624/2018-5 and the Sao Paulo Research Foundation (FAPESP) under grants 2013/20721-4, 2020/05865-3, 2022/02721-6 and 2022/00628-9.

T. A. Fagundes, L. J. R. Silva and R. Q. Machado are with the Sao Carlos School of Engineering, University of Sao Paulo, Sao Carlos SP 13566-590, Brazil (e-mail: thales.fagundes@usp.br; lucasjonys@usp.br; rquadros@sc.usp.br).

G. H. F. Fuzato is with the Federal Institute of Education, Science and Technology of Sao Paulo, Campinas SP 01109-010, Brazil (e-mail: guilherme.fuzato@ifsp.edu.br).

R. F. Q. Magossi is with Solar21, Sao Paulo, Brazil (e-mail: rafael.magossi@solar21.com.br)

J. C. Vasquez and J. M. Guerrero are with the Department of Energy Technology, University of Aalborg, 9220 Aalborg, Denmark (e-mail: juq@energy.aau.dk; joz@energy.aau.dk)

uncertainties for shipboard MGs [22] and also guarantee the operation in aerospace systems, military devices and medical equipment [23]. According to [24], dc/dc converters with parallel modules can increase the reliability due to the system redundancy, which interface RESs that operate with energy management system (EMS).

Therefore, this paper proposes a dc MG with redundancy similar to Fig. 1, then, a combination between cascaded bidirectional Cuk converter (CBC) and cascaded bidirectional Boost converter (CBB) that interface two BESSs as common input. The CBC is responsible to connect the dc-link, thus, it can provide a continuous current that affords a more stable dc-link voltage with load variation, while CBB is responsible to equalize the BESSs in a battery-to-battery (B2B) strategy. Later, the dc-link from CBC also connects the dc-utility by the use of a Boost converter. Thus, the dc MG operates to balance the SoC from the BESSs by using the SoC-sharing function proposed in [11].

As the SoC-sharing function can handle with load variations by changing its voltage level according to SoC, the suggested method is capable of effectively integrating with solar panels, wind power, and fuel cells, as presented in [11], which designed the SoC-sharing function for a common dc MG with the specific aim of mitigating load transitions that could potentially harm a fuel cell. Later, for the proposed approach in this manuscript, the redundancy from the cascaded modules can increase the dc MG reliability and guarantee the EMS efficiency.

Aiming at the stability analysis, the CBC and CBB are modelled as one topology and then coupled with the Boost converter model by the dc-link to calculate the complete dc MG average model which considers the SoC-sharing function and droop controller. Thus, the influence and interaction among the switches of CBB and CBC are not neglected when the stability analysis is addressed by using the Lyapunov's indirect method [25]. Therefore, the main contributions of the paper are listed as follows:

1) Incorporating redundancy into the dc MG can enhance its reliability during uncertain events;
2) The Cuk converter provides a more stable dc link voltage by maintaining continuous current on the dc load;
3) BESS-connected inductances divide current and reduce stress on components;
4) The CBB has the capability to accommodate dc loads on the secondary dc bus;
5) The SoC-sharing function is designed for charging and discharging the BESSs according to the EMS, while there are some strategies that the current references need to be set (positive or negative) for charging or discharging the BESSs, as proposed in [15], [18];
6) As the current reference cannot be zero during the equalization process in a system without dc load, the SoC-sharing can be used for B2B equalization in CBB;
7) No source communication is required for the EMS.

Finally, the paper is organized as follows. Section II the proposed dc MG is addressed. On that basis, Section III shows the EMS with the droop controller and SoC-sharing function. Later, in Section IV, the stability analysis by Lyapunov's indirect method proves the proposed approach. Section V presents the simulations via Matlab/Simulink and experimental results of the dc MG. Finally, the conclusion is given in Section VI.

II. DC MG CONFIGURATION

The proposed model that receives the EMS and the redundancy of SoC equalization is presented in Fig. 2. It is composed by a CBC, which is an association of two Cuk converters connected to the output common dc-link (on the capacitor C_o), and CBB, which is an integration of two bidirectional Boost converters tied to the capacitance C_3.

Both CBC and CBB share BESS1 and BESS2 as common input where BESS1 has its terminal voltage v_{bat1} connected to the inductances L_1 and L_5 which are flowing the currents i_{L1} and i_{L5} (with $i_{L1}+i_{L5}=i_{bat1}$). Considering BESS2, the terminal voltage v_{bat2} is connected to the inductances L_3 and L_6, with the BESS2 current defined as $i_{bat2}=i_{L3}+i_{L6}$.

Regarding the CBC, C_1 (with v_{C1} on its terminals) receives energy from BESS1, while C_2 (with v_{C2} on its terminals) absorbs energy from BESS2. In addition, L_2 and L_4 are the inductances which are flowing the currents i_{L2} and i_{L4}, while the dc-link voltage v_o is connected to the load R_o that absorbs/supplies current from each Cuk converter. In addition, controlled semiconductors S_1 and S_2 (with complementary PWM signals $\bar{S}_1$ and $\bar{S}_2$) are used in CBC, while switches S_3 and S_4 (with complementary PWM signals $\bar{S}_3$ and $\bar{S}_4$) are used in CBB.

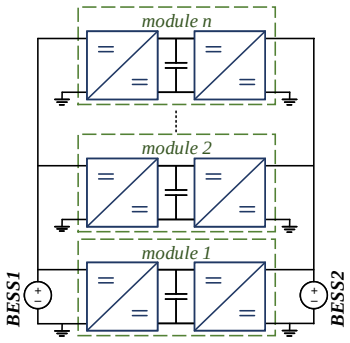

Fig. 1. Proposed dc MG with redundancy.

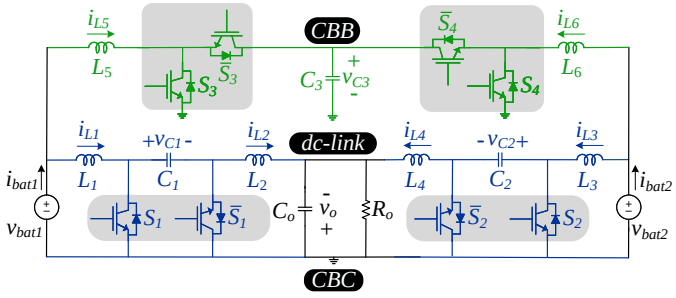

Fig. 2. Power converters (CBB and CBC) with two BESSs.

Regarding the operation of the model shown in Fig. 2, its complementary control signals allow for a continuous bidirectional power capability. Taking the CBB into account, it is responsible for transferring power directly from BESS1 to BESS2 (or from BESS2 to BESS1) without involving the dc-link. As a result, this module plays a crucial role in not factoring in the power demand on the dc-link during the EMS operation. In instances of high load steps in the dc-link, there can also be a power flow between BESS1 and BESS2 through CBB. Additionally, the CBC is capable of processing power from both BESSs to the dc-link (and also can charge both BESSs). The advantage of CBC lies in its ability to handle continuous current, making it suitable for loads that cannot undergo stress and require low current ripples [26].

III. EMS Methodology

An EMS plays a crucial role in managing RES, coordinating power flow, and maintaining system stability by monitoring load demand and ensuring the SoC equalization for BESSs [4]. Therefore, the redundancy-based SoC-sharing approach significantly enhances the operation of the MG, even under high load demand on the dc-link. As the dc MG operates to balance the SoC among the BESSs, a Boost converter is used to connect the common capacitance C_o to a dc-utility, which can maintain the dc-link voltage v_o, as shown in Fig. 3. In addition, each storage devices stack is composed by three sealed lead-acid BESSs in series connection, with 60 Ah of rated capacity and 12 V of nominal voltage (which result in 36 V per stack).

A. System control

The current references i_{L1_ref} and i_{L3_ref} are obtained from the SoC-sharing functions Sigmoid 1 and Sigmoid 2 which receive the SoC_1, SoC_2 and the dc-link voltage v_o to calculate the aforementioned current references through the inductances L_1 and L_3, respectively. Additionally, Sigmoid 3 and Sigmoid 4 are responsible to determine the current references i_{L5_ref} and i_{L6_ref} (through the inductances L_5 and L_6) by receiving as input the voltage v_{C3} on the capacitance C_3, SoC_1 and SoC_2, respectively.

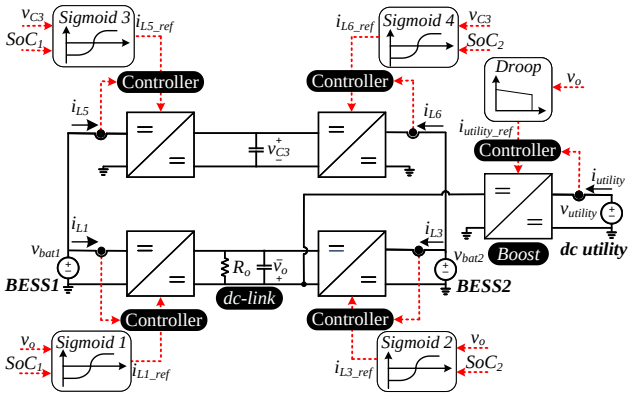

Fig. 3. Redundancy-based EMS to increase system reliability in SoC equalization.

Therefore, the system presents a redundancy which can enhance the reliability of the EMS, maintaining the SoC equalization, even though one of the cascaded modules are non-operating or under maintenance. In sequence, each current reference (i_{L1_ref}, i_{L3_ref}, i_{L5_ref} and i_{L6_ref}) are compared with the acquired currents through the inductances (i_{L1}, i_{L3}, i_{L5} and i_{L6}) to be processed through the classical PI controllers. Regarding the management applied on the dc-utility, the droop controller is the proposed solution to keep regulated the dc-link voltage, which receives v_o to define its current reference named $i_{utility\_ref}$. Later, the $i_{utility\_ref}$ is compared with the measured current through the utility $i_{utility}$ and then, processed through a PI controller.

Finally, the MG coordinates the power flow from the dc-utility and BESSs based on the redundancy in the SoC equalization, i.e., it is also important argue that SoC-sharing function operates with decentralized communication, thus each Sigmoid function only need to receive the information about its dc-link (local variable) and SoC (global variable).

B. Droop control for the dc-utility

The management of the dc-utility is performed by using a droop controller to keep its stability. In this procedure, the voltage v_o on dc-link determines the current reference i_{utiliy_ref}, as summarized in (1).

$$i_{utiliy\_ref} = i_{utiliy\_max}\left(-\frac{v_o}{\Delta v_o} + \frac{v_{set} + \Delta v_o}{\Delta v_o}\right) \quad (1)$$

Therefore, in (1) the term i_{utiliy_max} is the maximum current of the dc-utility, v_o is the dc-link voltage measured (even though the Cuk output voltage is negative, the voltage sensor is set to provide the absolute value in the experimental setup), v_{set} is the minimum dc-link voltage applied on droop controller and Δv_o is the voltage range. In addition, the virtual resistance that process the droop controller is also defined as $r_{virtual} = \Delta v_o / i_{utility\_max}$, and it is related to the level of slopping in the droop model.

C. Redundancy-based SoC-sharing approach

The SoC-sharing function is defined in [11] and this paper designs the methodology in the dc MG with redundancy to guarantee the decentralized SoC balancing among the BESSs, i.e., the solution does not require communication among BESSs and dc-utility. In Fig. 3, it is also noted that the CBB and CBC are responsible for the SoC equalization, concomitantly. Although the topology also accepts another dc load tied to C_3, for this project the CBB is responsible for B2B equalization among BESSs, i.e., there is not load tied to the capacitance C_3, thus one BESS transfer power to the other BESS, while the CBC also provide power to the dc load R_o connected to the dc-link.

1) Current references: In this context, the SoC-sharing functions are represented by Sigmoid 1 and 2 to calculate the current references i_{L1_ref} and i_{L3_ref} for the CBC, while Sigmoid 3 and 4 are responsible to define i_{L5_ref} and i_{L6_ref} for the CBB, respectively. In the end, the current reference

i_{L_ref} for each inductance (L_1, L_3, L_5 and L_6) written in a general form is illustrated in (2).

$$i_{L\_ref} = \frac{2}{1 + e^{(e_{factor} - SoC)p}} - 1 \tag{2}$$

Also in (2), the factor SoC can be defined as SoC_1 for i_{L1_ref} and i_{L5_ref} or SoC_2 for i_{L3_ref} and i_{L6_ref}.

In addition, e_{factor_vo} is the equalization factor represented in (3) for CBC, where v_o is the dc-link voltage, v_{set} is the minimum voltage on the dc-link and Δv_o is the voltage range (same parameters calculated from the droop controller).

$$e_{factor\_vo} = \frac{v_o - v_{set}}{\Delta v_o} \tag{3}$$

Furthermore, the Sigmoid function is designed to accommodate specific intervals: [-1 to 1] for BESS current (expressed in per unit (p.u.)), [0% to 100%] for SoC, and [v_{set} to v_{set} + Δv_o] for the voltage range on the dc-link. Consequently, the parameter p controls the slope of the curve within these intervals, as illustrated in Fig. 4(a), where the Sigmoid function slope is demonstrated for values of p equal to 5, 10, and 20. Hence, selecting p as 10 proves to be more suitable for the purpose of the equalization approach.

From Fig. 4(b), there is a relationship considering e_{factor_vo} as a function of the dc-link voltage (from 200 V to 220 V). Based on this analysis, a smooth equalization process takes place to mitigate MG instability when the e_{factor_vo} approaches zero. This is because the dc-link is nearing its maximum operational capacity, as evident from the minimum dc-link voltage. In contrast, achieving BESS balancing becomes effortless as v_o approaches 220 V, due to the low load demand on the dc-link.

Other important aspect is the 3-D surface produced by (2) (considering e_{factor_vo}) and illustrated in Fig. 5. In this picture, the SoC-sharing function calculates i_{L_ref} as a function of the v_o and the SoC with v_{set} = 200 V and Δv_o = 20 V. To understand the proposed solution, the authors evaluate (2) at two distinct situation: i_{L_ref} versus v_o, when different slices of SoC are analyzed, as shown in Fig. 6(a), and i_{L_ref} versus SoC, when different sections of v_o are analyzed according to Fig. 6(b).

Taking into account Fig. 6(a), SoC = 0% implies in the BESS charging process regardless the v_o level, while the BESSs fully charged provides power to the dc-link for the entire v_o range. Moreover, when the BESSs have intermediate values (between the boundaries), they can be charged or discharged according to the SoC range and v_o levels.

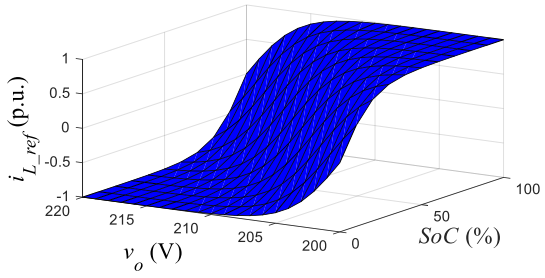

Fig. 5. SoC-sharing surface.

Considering Fig. 6(b), v_o = 200 V makes the BESSs operate in the discharging mode apart from the SoC, while high level dc-link voltage (v_o = 220 V) forces the BESSs absorb power from the dc-link for the entire SoC range. Moreover, when v_o is between the limits of operation, the charging or discharging modes are preferred according to the v_o range and SoC level.

As the SoC-sharing function can operate at the same voltage level as the droop controller, the proposed approach can be readily implemented and designed for integrating BESSs into a dc MG with other RES operating with a droop controller. Lastly, to maintain the SoC-sharing function within its boundaries, in cases where the current reference extends beyond these limits, the per unit current is adjusted to -1 for charging and 1 for discharging.

2) CBB-redundancy with B2B: Considering the CBB, the equalization factor e_{factor_vc3} is given in (4).

$$e_{factor\_vC3} = \frac{v_{C3} - v_{set\_C3}}{\Delta v_{C3}} \tag{4}$$

where v_{C3} is the voltage on C_3, v_{set_C3} is the minimum voltage and Δv_{C3} is the range of operation.

Although the currents $i_{L5\_ref} = -i_{L6\_ref}$ (neglecting the losses), the SoC-sharing needs to be designed for both inductances because the SoC_1 and SoC_2 define the voltage of equilibrium v_{C3} for the equalization process. In this type of procedure, the expected result is the B2B equalization according to the expression shown in (5).

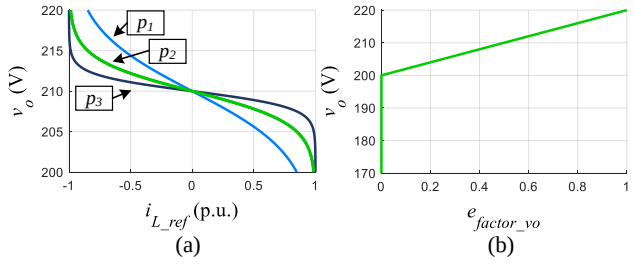

Fig. 4. SoC-sharing design parameters. (a) i_{L_ref} according to voltage level v_o, considering p equivalent to $p_1 = 5$, $p_2 = 10$ and $p_3 = 20$. (b) e_{factor} according to voltage level (v_o).

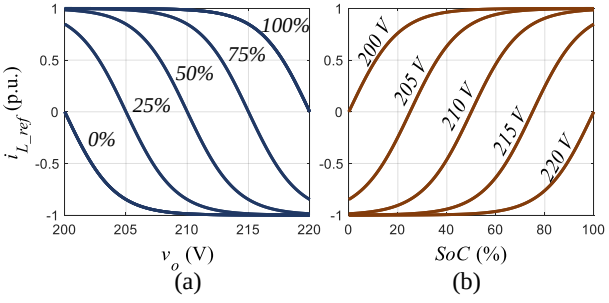

Fig. 6. SoC-sharing in 2-D. (a) i_{L_ref} as a function of v_o with constant SoC. (b) i_{L_ref} as a function of SoC with constant v_o.

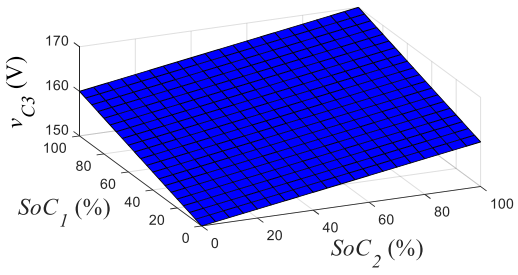

Fig. 7. Voltage v_{C3} as a function of SoC_1, SoC_2 and considering the B2B equalization designed for the CBB.

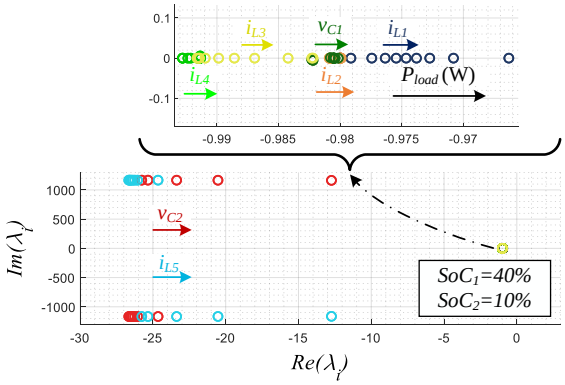

Fig. 8. Movement of eigenvalues in the complex plane considering the dc load variation.

$$\underbrace{\frac{2}{1+e^{(e_{factor\_vC3}-\mathrm{SoC}_1)p}}-1}_{i_{L5\_ref}}=-\underbrace{\left(\frac{2}{1+e^{(e_{factor\_vC3}-\mathrm{SoC}_2)p}}-1\right)}_{i_{L6\_ref}} \quad (5)$$

Later, taking into account the parity described in (5), a new expression calculated in (6) and plotted in Fig. 7 can be derived, which determines the voltage v_{C3} as a function of SoC_1, SoC_2, Δv_{C3} and v_{set_C3}, i.e., the CBB is operating in the B2B equalization mode.

$$v_{C3}=\left(\frac{\mathrm{SoC}_1+\mathrm{SoC}_2}{2}\right)\Delta v_{C3}+v_{set\_C3} \quad (6)$$

Finally, this topology with redundant module can increase the reliability, because it can guarantee the SoC equalization even if there is a high load demand connected to the dc-link (on C_o) reducing the SoC equalization capability that is operating on the CBC. As the CBB operates with the SoC-sharing function by using B2B equalization through the currents i_{L5} and i_{L6}, the BESS with lower SoC will receive current from the other BESS. Thus, as the expression (SoC_1 + SoC_2) has a light variation during the SoC equalization, the v_{C3} will maintain at same level by the influence of initial SoC from each BESS.

IV. Stability Analysis

This section evaluate the stability taking into account different scenarios by using the Lyapunov's indirect method which consider the complete EMS (SoC-sharing function and the droop controller) designed for the dc MG proposed by [25]. Thus, the interaction among the CBC, CBB and dc/dc utility converter are analyzed observing the movement of the eigenvalues obtained from the solution of the Jacobian's matrix in (7), and which parameters are defined in the Appendix.

In addition, the analytical model in (8) represents the influence of v_o from the dc/dc converters in the common dc-link, i.e., the dc-utility converter and CBC interactions. In the first scenario, it is considered the dc load variation and SoCs constants. Later, in the second case, the stability was evaluate with SoC equalization and dc-load constant. Subsequently, the SoC equalization and dc-load variations are accounted. Finally, the last case analyzed the impact of the maximum power delivery from the BESS units and dc-utility with the dc load and SoC constants.

A. First case: load variation on the dc-link

In the first case, the power variation performed on the load terminals from 100 W to 500 W (with $P_{load}=V_o^2/R_o$ being P_{load} and V_o the average power and voltage on the dc-link), when $\mathrm{SoC}_1=40\%$ and $\mathrm{SoC}_2=10\%$. As BESS1 is partially and BESS2 is totally discharged, both BESSs are forced to consume power from the dc-link. Although the eigenvalues are inside the stable region, the closest states to the right side of the complex-plan are i_{L1}, i_{L2}, i_{L3}, i_{L4} and v_{C1}, because BESS1 (SoC_1 = 40%) supplies much more power to the dc-link than BESS2 (SoC_2 = 10%), as shown in Fig. 8. Regarding i_{L5} and i_{L6}, the absence of load demand on the capacitor C_3 means that its influence on the stability is negligible. Finally, the dc-utility converter does not also impact the dc MG

$$\begin{bmatrix}\dot{v}_o\\ \dot{\boldsymbol{x}}_{cb}^{(1:9)}\\ \dot{e}_{iL1}\\ \dot{e}_{iL3}\\ \dot{e}_{iL5}\\ \dot{e}_{iL6}\\ \dot{\boldsymbol{x}}_{utility}^{(1:2)}\\ \dot{e}_{utility}\end{bmatrix}=\begin{bmatrix}dc_{coupled}\\ \boldsymbol{A_{cb}}(k_1,k_2,k_3,k_4)^{(1:9,1:10)}\boldsymbol{x_{cb}}+\boldsymbol{B_{cb}}(k_1,k_2,k_3,k_4)^{(1:9,1:2)}\boldsymbol{u_{cb}}\\ i_{L1\_ref}-Hi_{L1}i_{L1}\\ i_{L3\_ref}-Hi_{L3}i_{L3}\\ i_{L5\_ref}-Hi_{L5}i_{L5}\\ i_{L6\_ref}-Hi_{L6}i_{L6}\\ (\boldsymbol{A}_{utility10}^{(1,1:2)}+k_{utility}\boldsymbol{A}_{utilityk}^{(1,1:2)})\boldsymbol{x}_{utility}+(\boldsymbol{B}_{utility0}^{(1,1)}+k_{utility}\boldsymbol{B}_{utilityk}^{(1,1)})\boldsymbol{u}_{utility}\\ i_{utility\_ref}-Hi_{utility}i_{utility}\end{bmatrix} \quad (7)$$

$$dc_{coupled}=(\boldsymbol{A}_{cb}(k_1,k_2,k_3,k_4)^{(10,1:10)})\boldsymbol{x}_{cb}+(\boldsymbol{B}_{cb}(k_1,k_2,k_3,k_4)^{(10,1:10)})\boldsymbol{u}_{cb}-(\boldsymbol{A}_{utility0}^{(2,1:2)}+k_{utility}\boldsymbol{A}_{butilityk}^{(2,1:2)})\boldsymbol{x}_{utility}-(\boldsymbol{B}_{utility0}^{(2,1)}+k_{utility}\boldsymbol{B}_{utilityk}^{(2,1)})\boldsymbol{u}_{utility}-\left(-\tfrac{v_o}{R_oC_o}\right) \quad (8)$$

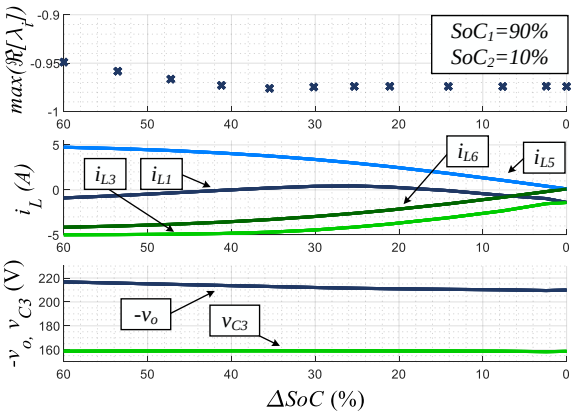

Fig. 9. Movement of the $max(Re(\lambda_i))$ considering the equalization process according to $\Delta SoC \rightarrow 0\%$, inductance current behavior (i_{L1}, i_{L3}, i_{L5} and i_{L6}), dc-link voltage v_o and voltage on the capacitance C_3 (v_{C3}).

stability because the real terms of their eigenvalues $Re(\lambda_i)$ are placed around -2,000, which does not cause any loss of stability, as shown in Fig. 8.

B. Second case: SoC equalization with constant dc load

For this scenario, the initial conditions consider SoC_1 = 90% and SoC_2 = 10% with a constant load demand on the common dc-link. As can be seen on Fig. 9, the level of stability is showed considering the maximum real part of the eigenvalues $max(Re(\lambda_i))$ as a function of ΔSoC with ΔSoC = SoC_1 - SoC_2. During the equalization process, the CBC provides power to the dc-link making the currents i_{L1} and i_{L3} flowing from the sources to the load, $\Delta SoC \rightarrow 0\%$ and $-v_o$ goes from 220 to 215 V.

Considering the CBB, as the B2B equalization is not impacted by the dc load, v_{C3} assumes a constant value, the currents i_{L5} and i_{L6} are responsible to enhance the SoC equalization in the complete operation of the dc MG with i_{L5} flowing from BESS1 to C_3, while i_{L6} flows from C_3 to BEES2. Finally, with ΔSoC = 0%, the SoC equalization was achieved and, consequently, i_{L1} = i_{L3} and i_{L5} = i_{L6}.

C. Third case: SoC equalization process with dc load variation

The third case, the authors apply the SoC equalization with dc load variation. In this type of procedure, Fig. 10 shows the load applied on the dc-link as a function of $max(Re(\lambda_i))$, ΔSoC(%) and considering initial conditions as SoC_1 = 90% and SoC_2 = 10%. For this scenario, the load starts at 150 W, and increments of 50 W are added until it reaches 1,300 W. According to Fig. 10, the dc MG is stable when the maximum P_{load} is lower than 750 W because the $max(Re(\lambda_i))$ remains confined in the left-side of the complex-plan.

D. Fourth case: evaluation of power contribution from BESS and dc-utility

In the last scenario, the power variation was applied from BESS units ($P_{BESS1} + P_{BESS1}$) starting from 0 W and it is increased to 500 W, along with dc utility ($P_{utility}$) also ranging from 0 W to 500 W. Additionally, the power applied on the dc-link is 200 W, with SoC_1 = 90% and SoC_2 = 60%. For this scenario, the dc MG remains stable when the total power produced by the BESSs and dc utility is not higher than the power demanded by the load, thus ensuring that $max(Re(\lambda_i))$ is lower than zero, as illustrated in Fig. 11.

V. Experimental Results

In this paper, the results were obtained in the real-time hardware-in-the-loop (HIL) with the interaction between Typhoon HIL (where the dc MG is built) and dSPACE system (where the control algorithms are embedded) made possible through a Printed Circuit Board (PCB), as illustrated in Fig. 12. The parameters from the redundancy-based dc MG are described in Table I, where the authors are including the parasitic losses for the entire power plant with $r_{L1}, r_{L2}, r_{L3}, r_{L4}, r_{L5}, r_{L6}$ and $r_{Lutility}$ representing the inductances losses, $r_{S1}, r_{\bar{S}1}, r_{S2}, r_{\bar{S}2}, r_{S3}, r_{\bar{S}3}, r_{S4}, r_{\bar{S}4}$ and $r_{Sutility}$ being the semiconductor losses, $r_{Dutility}$ meaning the diode loss in the dc-utility converter and finally, r_{C1}, r_{C2}, r_{C3} and r_{Co} acting as the capacitance losses.

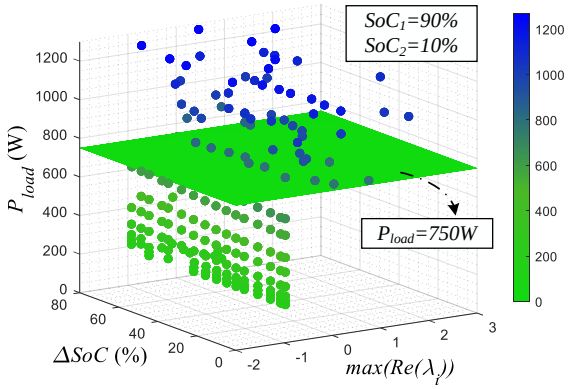

Fig. 10. Load variation on the dc-link as a function of $max(Re(\lambda_i))$ and the equalization process when $\Delta SoC \rightarrow 0\%$.

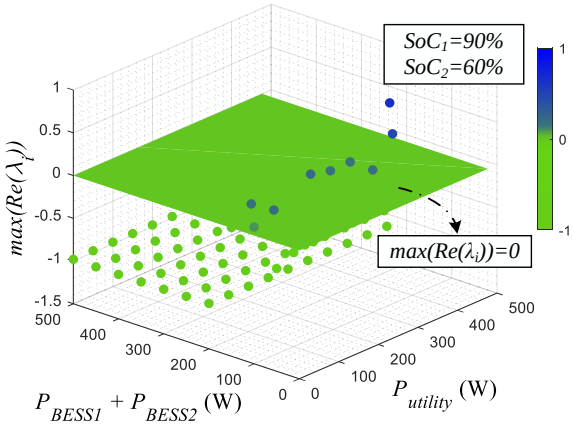

Fig. 11. $max(Re(\lambda_i))$ as a function of the total power from BESS units and dc-utility.

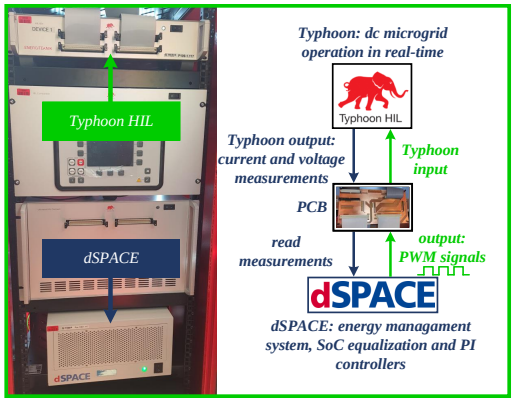

Fig. 12. Lab-scale prototype.

TABLE I
DC MG PARAMETERS

Component	***Value***
Inductances (L_1, L_2, L_3, L_4, L_5, L_6)	4.8 mH
Inductances ($L_{utility}$)	4.8 mH
C_1 and C_2	130 μF
C_3 and C_o	470 μF
Parasitic Losses	***Value***
$r_{L1} = r_{L2} = r_{L3} = r_{L4} = r_{L5} = r_{L6}$	150 $m\Omega$
$r_{Lutility}$	150 $m\Omega$
$r_{S1} = r_{S2} = r_{S3} = r_{S4} = r_{\bar{S}1} = r_{\bar{S}2} = r_{\bar{S}3} = r_{\bar{S}4}$	30 $m\Omega$
$r_{Sutility} = r_{Dutility}$	30 $m\Omega$
$r_{C1} = r_{C2}$	30 $m\Omega$
$r_{C3} = r_{CO}$	150 $m\Omega$

Additionally, a dc source with 36 V and 500 W as rated voltage and power is connected to the dc-utility input converter, as well as, two groups of batteries with each one having a rated capability of 60 Ah, rated voltage as 36 V and maximum current supplied/absorbed as 10 A from the BESSs. Aiming at the voltage range, the $-v_o$ is set from 200 to 220 V and v_{C3} is set from 150 to 170 V, Finally, the switching frequency is 10 kHz and the overall efficiency of the proposed method is 95%.

A. Comparison between experimental and simulation tests performed via Matlab/Simulink

For this first test, the BESS capacities were reduced by a factor of 500 to speed up the SoC balancing, with initial values as $\text{SoC}_1 = 40\%$ and $\text{SoC}_2 = 10\%$. In Fig. 13, the authors compare the experimental results with simulations performed via Matlab/Simulink with steps of load ($\Delta P_{Load} \approx 130$ W). In this context, the behavior of dc-link voltage ($-v_o$), v_{C3}, BESS currents (i_{bat1} and i_{bat2}), the inductance currents (i_{L1}, i_{L3}, i_{L5} and i_{L6}) are shown. According to the operation, the elapsed time to achieve the balancing is around 35 s even with steps of load ($\Delta P_{Load} \approx 130$ W) performed on the dc-link. This demonstrates that there is no significant discrepancy between experimental results and Matlab/Simulink simulations when the authors are evaluating SoC_1 and SoC_2.

Considering that load maneuvers are performed on the dc-link, the currents through the inductances i_{L1} and i_{L3} are modified to maintain the voltage v_o inside the limits

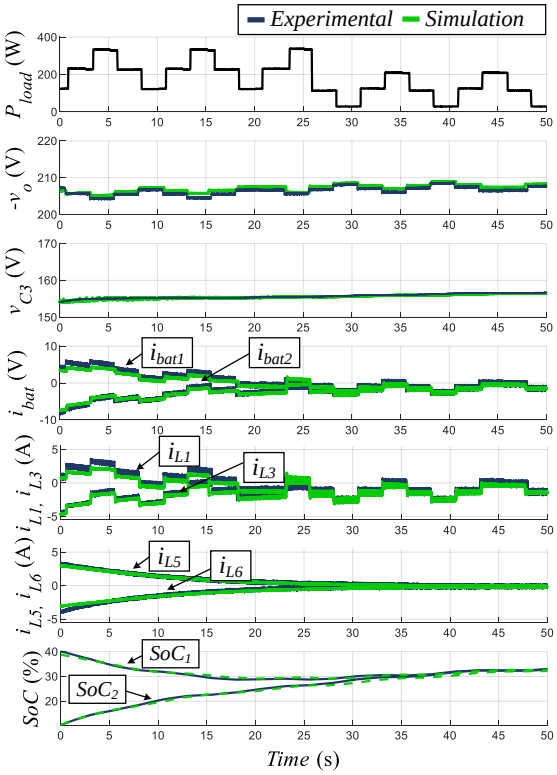

Fig. 13. Comparison between experimental setup and simulations via Matlab/Simulink. Initial $\text{SoC}_1 = 40\%$ and $\text{SoC}_2 = 10\%$.

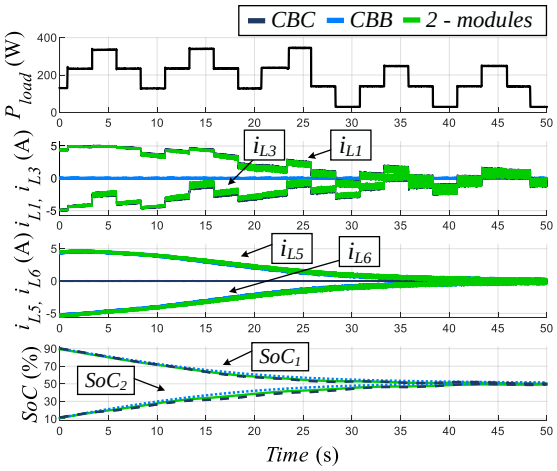

Fig. 14. SoC equalization considering only the CBC, the CBB and the 2 modules operating simultaneously in the lab-scale prototype.

of operation, while i_{L5} and i_{L6} are responsible to enhance the SoC equalization. As a result, the dc MG configuration achieves the SoC equalization even when a high amount of power (dc load is changed) is maneuvered on the dc-link ($-v_o \approx 205$ V).

B. Reliability evaluation during the SoC equalization

In order to assess the reliability of the dc MG, the equalization process was analyzed as a performance criterion, taking

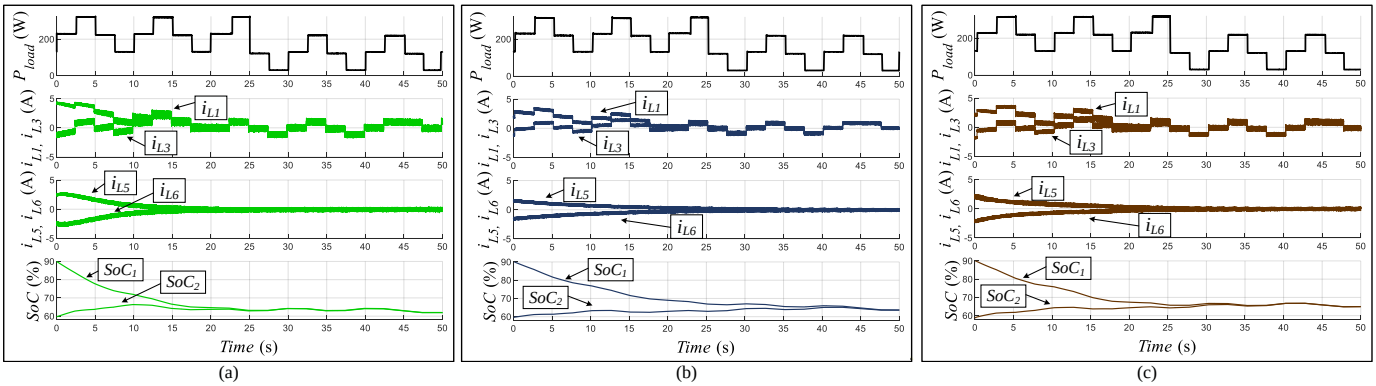

Fig. 15. Comparison among the EMS (experimental tests). (a) SoC-sharing function. (b) SoC-based droop. (c) Fuzzy method.

into account either only the CBC, only the CBB, and both modules operating together, as shown in Fig. 14, with steps of load turned-on and off on the dc-link ($\Delta P_{Load} \approx 130$ W), SoC starting at 90% for BESS1 and at 10% for BESS2.

To understand the effectiveness of the proposed approach, the regime of working were considered: the BESS capacities were reduced by a factor of 500 when only one module (CBB or CBC) is performing the SoC equalization, while their capacities were decreased by a factor of 250 when both (CBC and CBB) are accomplishing the SoC balancing. Therefore, as the configuration has redundancy, the SoC equalization is achieved more effectively in case of multiple module under operation. Thus, if the dc MG has more than two modules connected, the redundancy increases the reliability of the EMS.

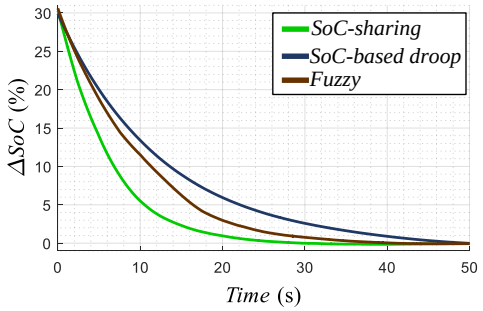

Fig. 16. Time of equalization considering the SoC-sharing function, SoC-based droop and Fuzzy method.

C. Comparison with other strategies applied in the proposed dc MG

In this section, the results are performed to compare the SoC-sharing approach with other methodologies found in the literature. At first, [15] presented an EMS utilizing battery Ampere-hour capacity without droop control. Nevertheless, this method is unsuitable for CBB module if the capacitor C_3 has no load, because the EMS generates non-zero current references that lead to imbalanced BESSs. Later, the authors try to apply the SoC-based droop proposed by [18] as comparable technique, however, it is unaccepted because this methodology does not work properly when no load is tied to the capacitor on C_3.

Subsequently, as the SoC-based droop proposed in [20] has flexibility to modify the rated voltage on C_3 when no load is tied to its terminals, it is suitable for B2B strategy on CBB and a viable technique used as method of comparison. Furthermore, the approach proposed by [16] was also implemented, where SoC balance is achieved through the use of Fuzzy controllers. Since the Fuzzy controller operates with SoC and dc-link voltage as inputs and provides the reference current, this solution is also well-suited for B2B equalization in CBB when there is no load tied to C_3.

To understand the process of evaluation, by alternating the activation and deactivation of load increments on the dc-link ($\Delta P_{Load} \approx 130$ W), Fig. 15 shows the comparison among SoC-sharing function (Fig. 15(a)), SoC-based droop designed according to [20] (Fig. 15(b)) and Fuzzy as proposed by [16] (Fig. 15(c)). As can be seen, although the strategies show similar performance, the SoC-sharing function is faster according to Fig. 16. This occurs because the SoC-sharing produces higher current levels at the same voltage when it is compared to SoC-based droop and Fuzzy methods. Finally, Table II provides information regarding the time response for ΔSoC when it is decreased in steps of 5% until SoC equalization is achieved for SoC-sharing function, SoC-based droop, and Fuzzy methods. Therefore, according to i_{L5} and i_{L6}, the suggested approach offers marginally greater efficacy on CBB with the B2B strategy. To conclude, the SoC-sharing function exhibits superior performance in the proposed redundancy-based dc MG.

TABLE II
COMPARING AMONG OTHER METHODOLOGIES: THE TIME IT TAKES FOR ΔSOC TO DECREASE BY 5% INCREMENTS UNTIL IT REACHES 0%.

ΔSoC	*SoC-sharing function*	*SoC-based droop*	*Fuzzy*
25%	1.31 s	2.2 s	2.0 s
20%	2.7 s	5.0 s	4.4 s
15%	4.5 s	8.5 s	7.2 s
10%	6.8 s	13.5 s	11.3 s
5%	10.5 s	22.0 s	16.4 s
0%	30.1 s	50.0 s	45.0 s

VI. Conclusion

In this paper, a modified redundancy-based EMS for MGs was proposed, which involved designing an SoC-sharing function to balance the SoC of BESSs. The proposed dc MG is composed by a combination between CBC and CBB that interface the BESS, while a dc/dc Boost connects the dc-utility to the common dc-link. As a result of this configuration, if the dc MG face electrical faults or maintenance, the operation can continue to balance the SoC. Thus, the SoC-sharing function is addressed with B2B equalization on CBB and with a contribution of power to the dc load. As a result, this dc MG can be applied in system that electrical uncertainties events can unbalancing the BESSs, but must continue provide power according to load demand. Then, B2B equalizes the BESS in the CBB module, while CBC provides more stable voltage on dc-link.

Firstly, the SoC-sharing function was presented, then the Lyapunov's indirect method addressed that the proposed configuration is stable, taking into account a power demand of 750 W applied to the dc-link, each BESS unit having a capacity of 250 W and the dc-utility rated at 500 W. In sequence, an experimental setup along with simulations via Matlab/Simulink evaluate the performance of the proposed algorithm to prove the feasibility of the methodology designed for MGs. The comparison with other methodologies revealed the following results: using the SoC-sharing function, the SoC difference among BESS units takes 10.5 seconds to reach 5% and 30.1 seconds to achieve equalization. On the other hand, in a SoC-based droop control scheme, it takes 22.0 seconds to reach 5% SoC difference and 50 seconds to achieve equalization. Additionally, using a the Fuzzy approach, it takes 16.4 seconds to reach 5% of SoC difference and 45 seconds to attain balance. In conclusion, the proposed redundancy-based dc MG proves to be more suitable for operation when utilizing the suggested SoC-sharing function.

Appendix
Nomenclature from the complete dc MG model

$\boldsymbol{x}_{cb}$: state vector of CBC and CBB modelled as one topology with $\begin{bmatrix} i_{L1} & i_{L2} & v_{C1} & i_{L3} & i_{L4} & v_{C2} & i_{L5} & i_{L6} & v_{C3} & v_o \end{bmatrix}^T$;
$\dot{\boldsymbol{e}}_{iL1}$, $\dot{\boldsymbol{e}}_{iL3}$, $\dot{\boldsymbol{e}}_{iL5}$, $\dot{\boldsymbol{e}}_{iL6}$ and $\dot{\boldsymbol{e}}_{utility}$: error of currents $\dot{e}_{iL} = i_{L\_ref} - i_L$ and $\dot{e}_{utility} = i_{utility\_ref} - i_{utility}$;

$\boldsymbol{u}_{cb}$ and $\boldsymbol{u}_{utility}$: input vectors of CBC and CBB modelled as one topology and utility converters defined as $\begin{bmatrix} v_{bat1} & v_{bat2} & v_o \end{bmatrix}^T$ and $\begin{bmatrix} v_{utility} \end{bmatrix}^T$;

$\boldsymbol{x}_{utility}$: utility state vector defined as $\begin{bmatrix} i_{utility} & v_o \end{bmatrix}^T$;

$\boldsymbol{A}_{cb}(k_1, k_2, k_3, k_4)$: state space from the model on Fig. 2 as a function of the PWM duty cycles k_1, k_2, k_3 and k_4 applied on the switches (S_1, S_2, S_3 and S_4). The matrix indices (1:9,1:10) avoid the parameters related to $\dot{v}_o$, while (10,1:10) considered them;

$\boldsymbol{B}_{cb}(k_1, k_2, k_3, k_4)$: input matrix with indices as (1,1) to select the parameters related to $\dot{v}_o$, while (2,1) avoid the terms related to them;

$\boldsymbol{A}_{utility} = \boldsymbol{A}_{utility0} + k_{utility}\boldsymbol{A}_{utilityk}$: state space model of utility. The matrix indices (1,1:2) select the parameters related to dc-link voltage, while (2,1:2) avoid them;

$\boldsymbol{B}_{utility} = \boldsymbol{B}_{utility0} + k_{utility}\boldsymbol{B}_{utilityk}$: input matrix of utility with indices as (2,1) to avoid the parameters related to $\dot{v}_o$, while (1,1) consider them;

Hi_{L1}, Hi_{L3}, Hi_{L5}, Hi_{L6} and $Hi_{utility}$: current gain sensors;

$\left(-\frac{v_o}{R_o C_o}\right)$: integration of the dc-utility and CBC converters.

References

[1] S. A. Hasib, S. Islam, R. K. Chakrabortty, M. J. Ryan, D. K. Saha, M. H. Ahamed, S. I. Moyeen, S. K. Das, M. F. Ali, M. R. Islam, Z. Tasneem, and F. R. Badal, "A comprehensive review of available battery datasets, rul prediction approaches, and advanced battery management," *IEEE Access*, vol. 9, pp. 86 166–86 193, 2021.

[2] M. T. Lawder, B. Suthar, P. W. C. Northrop, S. De, C. M. Hoff, O. Leitermann, M. L. Crow, S. Santhanagopalan, and V. R. Subramanian, "Battery energy storage system (bess) and battery management system (bms) for grid-scale applications," *Proceedings of the IEEE*, vol. 102, no. 6, pp. 1014–1030, 2014.

[3] T. L. Zhang, Q. Zhou, S. Mu, H. Li, Y. J. Li, and J. Wang, "Voltage-based segmented control of superconducting magnetic energy storage for transient power fluctuation suppression in island dc microgrid," *IEEE Transactions on Applied Superconductivity*, vol. 31, no. 8, pp. 1–5, 2021.

[4] C. R. de Aguiar, G. H. F. Fuzato, R. Q. Machado, and J. M. Guerrero, "An adaptive power sharing control for management of dc microgrids powered by fuel cell and storage system," *IEEE Transactions on Industrial Electronics*, vol. 67, no. 5, pp. 3726–3735, 2020.

[5] P. Chen, F. Xiao, J. Liu, Z. Zhu, and Q. Ren, "Unbalanced operation principle and fast balancing charging strategy of a cascaded modular multilevel converter–bidirectional dc–dc converter in the shipboard applications," *IEEE Transactions on Transportation Electrification*, vol. 6, no. 3, pp. 1265–1278, 2020.

[6] G. Shi, H. Han, Y. Sun, Z. Liu, M. Zheng, and X. Hou, "A decentralized soc balancing method for cascaded-type energy storage systems," *IEEE Transactions on Industrial Electronics*, vol. 68, no. 3, pp. 2321–2333, 2021.

[7] J. Lang, C. Zhang, F. Xia, G. Wang, and X. Wang, "Self-disciplined nonsmooth coordination control for battery energy storage system in autonomous dc microgrids toward large-signal stability," *IEEE Transactions on Smart Grid*, vol. 14, no. 2, pp. 928–938, 2023.

[8] N. L. Díaz, A. C. Luna, J. C. Vasquez, and J. M. Guerrero, "Centralized control architecture for coordination of distributed renewable generation and energy storage in islanded ac microgrids," *IEEE Transactions on Power Electronics*, vol. 32, no. 7, pp. 5202–5213, 2017.

[9] N. L. Díaz, J. C. Vasquez, and J. M. Guerrero, "A communication-less distributed control architecture for islanded microgrids with renewable generation and storage," *IEEE Transactions on Power Electronics*, vol. 33, no. 3, pp. 1922–1939, 2018.

[10] W. Jiang, C. Yang, Z. Liu, M. Liang, P. Li, and G. Zhou, "A hierarchical control structure for distributed energy storage system in dc micro-grid," *IEEE Access*, vol. 7, pp. 128 787–128 795, 2019.

[11] T. A. Fagundes, G. H. F. Fuzato, C. R. De Aguiar, K. D. A. Ottoboni, M. Biczkowski, and R. Q. Machado, "Management and equalization of energy storage devices for dc microgrids using a soc-sharing function," *IEEE Access*, vol. 8, pp. 78 576–78 589, 2020.

[12] N. Ghaeminezhad, Q. Ouyang, X. Hu, G. Xu, and Z. Wang, "Active cell equalization topologies analysis for battery packs: A systematic review," *IEEE Transactions on Power Electronics*, vol. 36, no. 8, pp. 9119–9135, 2021.

[13] Y. Cao, K. Li, and M. Lu, "Balancing method based on flyback converter for series-connected cells," *IEEE Access*, vol. 9, pp. 52 393–52 403, 2021.

[14] M. Uno and K. Yoshino, "Modular equalization system using dual phase-shift-controlled capacitively isolated dual active bridge converters to equalize cells and modules in series-connected lithium-ion batteries," *IEEE Transactions on Power Electronics*, vol. 36, no. 3, pp. 2983–2995, 2021.

[15] R. Bhosale, R. Gupta, and V. Agarwal, "A novel control strategy to achieve soc balancing for batteries in a dc microgrid without droop control," *IEEE Transactions on Industry Applications*, vol. 57, no. 4, pp. 4196–4206, 2021.

[16] T. A. Fagundes, G. H. F. Fuzato, P. G. B. Ferreira, M. Biczkowski, and R. Q. Machado, "Fuzzy controller for energy management and soc equalization in dc microgrids powered by fuel cell and energy storage units," *IEEE Journal of Emerging and Selected Topics in Industrial Electronics*, vol. 3, no. 1, pp. 90–100, 2022.
[17] N. Zhi, K. Ding, L. Du, and H. Zhang, "An soc-based virtual dc machine control for distributed storage systems in dc microgrids," *IEEE Transactions on Energy Conversion*, vol. 35, no. 3, pp. 1411–1420, 2020.
[18] T. R. Oliveira, W. W. A. Gonçalves Silva, and P. F. Donoso-Garcia, "Distributed secondary level control for energy storage management in dc microgrids," *IEEE Transactions on Smart Grid*, vol. 8, no. 6, pp. 2597–2607, 2017.
[19] G. Tian, Y. Zheng, G. Liu, and J. Zhang, "Soc balancing and coordinated control based on adaptive droop coefficient algorithm for energy storage units in dc microgrid," *Energies*, vol. 15, no. 8, 2022. [Online]. Available: https://www.mdpi.com/1996-1073/15/8/2943
[20] Y. Xia, M. Yu, P. Yang, Y. Peng, and W. Wei, "Generation-storage coordination for islanded dc microgrids dominated by pv generators," *IEEE Transactions on Energy Conversion*, vol. 34, no. 1, pp. 130–138, 2019.
[21] K. Bi, W. Yang, D. Xu, and W. Yan, "Dynamic soc balance strategy for modular energy storage system based on adaptive droop control," *IEEE Access*, vol. 8, pp. 41 418–41 431, 2020.
[22] S. Fang, Y. Xu, H. Wang, C. Shang, and X. Feng, "Robust operation of shipboard microgrids with multiple-battery energy storage system under navigation uncertainties," *IEEE Transactions on Vehicular Technology*, vol. 69, no. 10, pp. 10 531–10 544, 2020.
[23] R. Faraji, L. Ding, T. Rahimi, and M. Kheshti, "Application of soft-switching cell with inherent redundancy properties for enhancing the reliability of boost-based dc–dc converters," *IEEE Transactions on Power Electronics*, vol. 36, no. 11, pp. 12 342–12 354, 2021.
[24] W. Zhang, D. Xu, P. N. Enjeti, H. Li, J. T. Hawke, and H. S. Krishnamoorthy, "Survey on fault-tolerant techniques for power electronic converters," *IEEE Transactions on Power Electronics*, vol. 29, no. 12, pp. 6319–6331, 2014.
[25] G. H. F. Fuzato, C. R. de Aguiar, T. A. Fagundes, W. C. Leal, J. C. Vasquez, J. M. Guerrero, and R. Q. Machado, "Droop k-sharing function for energy management of dc microgrids," *IEEE Journal of Emerging and Selected Topics in Industrial Electronics*, vol. 2, no. 3, pp. 257–266, 2021.
[26] H.-T. Yang, H.-W. Chiang, and C.-Y. Chen, "Implementation of bridgeless cuk power factor corrector with positive output voltage," *IEEE Transactions on Industry Applications*, vol. 51, no. 4, pp. 3325–3333, 2015.

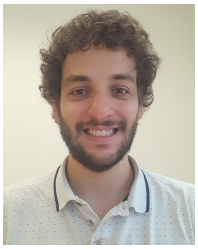

Thales Augusto Fagundes was born in Jundiai, Brazil. He received the B.S. in electrical engineering in 2017 and the M.S. degree in 2020 from the University of Sao Paulo (Sao Carlos, Brazil). In 2014, he studied abroad at the University of New South Wales (Sydney, Australia), focusing on courses related to alternative energy sources. He is currently working on his Ph.D. in electrical engineering at the University of Sao Paulo and from 2022 to 2023 he was a visiting researcher at the Aalborg University. His main research interest are in the fields of microgrids, energy management and DC-DC converters for renewable energy sources and storage systems.

Guilherme Henrique Favaro Fuzato was born in Varginha, Brazil, in 1989. He received the B.S. in Electrical Engineering in 2011, the M.S. degree in Power Electronics and Dynamic Systems in 2015, and the Ph.D. degree in Microgrids in 2019 from University of Sao Paulo. From 2018 to 2019 he was a visiting researcher at the University of Aalborg. From 2012 to 2013 he worked at Siemens as a field service engineer in automation area. From 2014 to 2015 he worked at Bosch with power electronics in automotive applications as a temporary researcher. Since 2016, he has been working as lecturer at the Federal Institute of Education, Science and Technology of Sao Paulo. His main research interests are in the fields of microgrids, energy management and dc/dc converter for renewable energy sources and storage systems.

Rafael Fernando Quirino Magossi received the B.Eng., M.Sc. and Ph.D. degrees in electrical engineering from the University of Sao Paulo, Sao Carlos, Brazil, in 2016, 2018 and 2020, respectively. From 2018 to 2022, he was an assistant professor at the Federal Center for Technological Education (CEFET/RJ) in Rio de Janeiro, Brazil. Since 2022, he has been the CTO at Solar21 in Sao Paulo, Brazil. His research interests include control systems, power electronics, and renewable power systems.

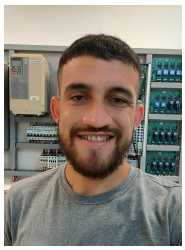

Lucas Jonys Ribeiro Silva received the B.S. in electrical engineering in 2020 from The Federal University of Viçosa and the M.S. degree in 2022 from the University of Sao Paulo. He is currently working on his Ph.D. in electrical engineering at the University of Sao Paulo. His main research interest are in the fields of microgrids, electric and hybrid vehicles, energy management and dc/dc converters for renewable energy sources and storage systems.

Juan C. Vasquez (Senior Member, IEEE) received the B.Sc. and Ph.D. degrees from UAM, Colombia, and the Ph.D. degree from UPC, Spain. In 2019, he was a Professor of energy internet and microgrids. He is currently the Co-Director of the Villum Center for Research on Microgrids. He has published more than 450 journal articles cited more than 30000 times. His research interests include operation, control, energy management applied to ac/dc microgrids, the integration of IoT, energy internet, digital twin, and blockchain solutions. He has been awarded as a Highly Cited Researcher, since 2017. He was a recipient of the Young Investigator Award, in 2019.

Josep M. Guerrero (Fellow, IEEE) received the B.S. degree in telecommunications engineering, the M.S. degree in electronics engineering, and the Ph.D. degree from the Technical University of Catalonia, Barcelona, in 1997, 2000, and 2003, respectively. In 2019, he was a Villum Investigator at the Villum Fonden, which supports the Center for Research on Microgrids (CROM), Aalborg University, Denmark. Since 2011, he has been a Full Professor with the Department of Energy Technology, Aalborg University. His research interests include different microgrid aspects, including applications as remote communities, energy prosumers, and maritime and space microgrids.

Ricardo Quadros Machado (M'2005, SM'2018) was born in Santa Maria, Brazil. He received the B. S. from the University of Santa Maria (Santa Maria, Brazil) in 1997, the M.S. (2000) and the Ph.D. (2005) degrees in Electrical Engineering from the University of Campinas (Campinas, Brazil). From 2002 to 2003 he was a visiting researcher at the University of Padova (Padova, Italy) and from 2005 to 2007 he was a post-doctorate at the Federal University of Santa Maria, (Santa Maria, Brazil). From 2013 to 2014 he was visiting professor at the University of Toronto (Toronto, Canada). Additionally, from 2007 to 2018 he was assistant professor at the University of Sao Paulo (Sao Carlos, Brazil). Currently, he is associated professor at the University of Sao Paulo (Sao Carlos, Brazil) and his main research interests are: processing of energy in dc/dc and dc/ac converters, digital control of power converters, distributed generation systems, smart grids and control of renewable energy sources.